# Acoustic emission characterization of the fracture process in steel fiber reinforced concrete

Xiong Zhou, Yuyou Yang[*], Xiangqian Li and Guoqing Zhao

*School of Engineering and Technology, China University of Geosciences (Beijing), Beijing 10083, China*

**Abstract.**  The correlation between the characteristics of acoustic emission signals and the strength parameters of concretes is investigated by combining the acoustic emission (AE) technique and steel fiber reinforced concrete (SFRC). By means of AE detection system, three kinds of steel fibers of varying content were used as reinforcement in concrete and their influence on the fracture process and the acoustic activity was considered in this paper. Analysis of the AE test results revealed that for different steel fiber contents, the role of steel fiber is different. Concave-convex steel fiber has an inhibitory effect on the control of crack expansion. Bow steel fiber has a better effect on the control of crack propagation when the fiber content is lower. The compressive strength of SFRC decrease when bow steel fiber content rises. Ultra-short can prevent early cracks of concrete.

**Keywords**:  acoustic emission; steel fiberreinforced concrete; steel fiber content; AE events column graph

## 1. Introduction

Deformation or crack will turn up in solid materials interior undergoing internal forces or external loads, as part of the strain energy being released in the form of sound waves which is generally characterized by acoustic emission (AE). The AE technique can be used to analyze the characteristics of elastic waves, which converted from sound waves that caused by microscopic damage in the material interior, by means of surface AE sensors to record the transient waves (hits) generated by the crack propagation incidents inside the material. This technique has been employed to assess the damage in important concrete structures, such as bridges, airport pavements and so on (Gholizadeh *et al*. 2015).

Steel fiber reinforced concrete (SFRC) is being increasingly employed in structural engineering. Fibers can restrain the occurrence of the early age cracking and limit the expansion of the crack, and contribute to improving concrete tensile and flexural strength, fatigue life, ductility and surface skin resistance (Shah and Ribakov 2011). Compared with common concrete, SFRC has good tensile property, bending performance and impact resistance. AE detection system has always been applied to clarify the physical and mechanical properties during uniaxial compression

---

[*]Corresponding author, Ph.D., E-mail: yangyuyou@cugb.edu.cn

tests and three-point bending tests on SFRC specimens (Aggelis *et al*. 2013).

The modern acoustic emission instruments were invented in 1960s, after which significant efforts have been made to utilize the AE technique to detect the damage characterization of solid materials (Bentahar and Gouerjuma 2009; Sagar and Prasad 2012; Carpinteri *et al*. 2013; Siracusano *et al*. 2016). Wu *et al*. (2000) carried out a series of tests to study the AE signal section and the failure mechanism of mortar, concrete and SFRC beams. Experimental results indicated that there exist nine distinct failure mechanisms for SFRC during the entire fracture process. Carpinteri *et al*. (2016) carried out three-point bending tests of concrete and observed that the dissipation energy rate rapidly increases and reaches its maximum value around the peak load. Ohtsu *et al*. (2002) proposed a practice for in situ monitoring of concrete structures by acoustic emission based on the Kaiser effect. Localization of AE events in D2 beam Alam *et al*. (2014) researched fracture character of concrete beams by localization of AE events and find that the formation of fracture starts before the maximum load is reached. Studies by Colombo *et al*. (2003) showed that micro cracks emit waves with smaller amplitudes, whereas the waves from macro cracks have larger amplitudes. Soulioti *et al*. (2009) studied the influence of varying content of steel fibers on the fracture process and the acoustic activity. Analysis revealed that particular AE parameters changed monotonically with the progress of damage and can be used to characterize the failure process. Aggelis *et al*. (2010) adopted the broadband sensors to capture a wide range of fracturing phenomena of SFRC, the experiments were conducted in four-point bending with concurrent monitoring of AE signals. The results indicated that AE parameters undergo significant changes much earlier than the final fracture of the specimens. It was suggested that proper study of AE parameters enabled the characterization of structural health of large structures in cases where remote monitoring was applied. Aggelis *et al*. (2011) thought acoustic emission can be used as a warning against the failure of this material while the broadband transducers can be used to characterize the different damage mechanisms.

In this study, three kinds of steel fiber were used as reinforcement in concrete, and for each kind of fiber, three different contents were considered. By means of the uniaxial compression tests and AE detection tests, the AE signals from all kinds of specimens were recorded. For each kind of specimen, AE events column graph was presented and analyzed.

## 2. Experiment setup

### 2.1 AE Detection system

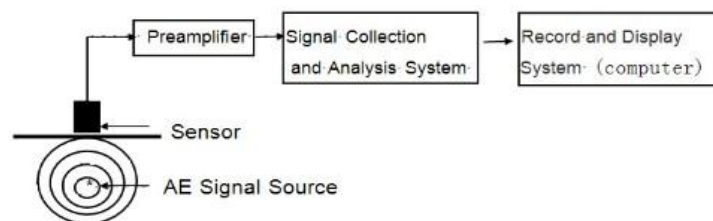The SAEU2S acoustic emission instrument produced by Beijing Shenghua Corporation was



Fig. 1 AE detection system

Fig. 2 The appearance of sensor

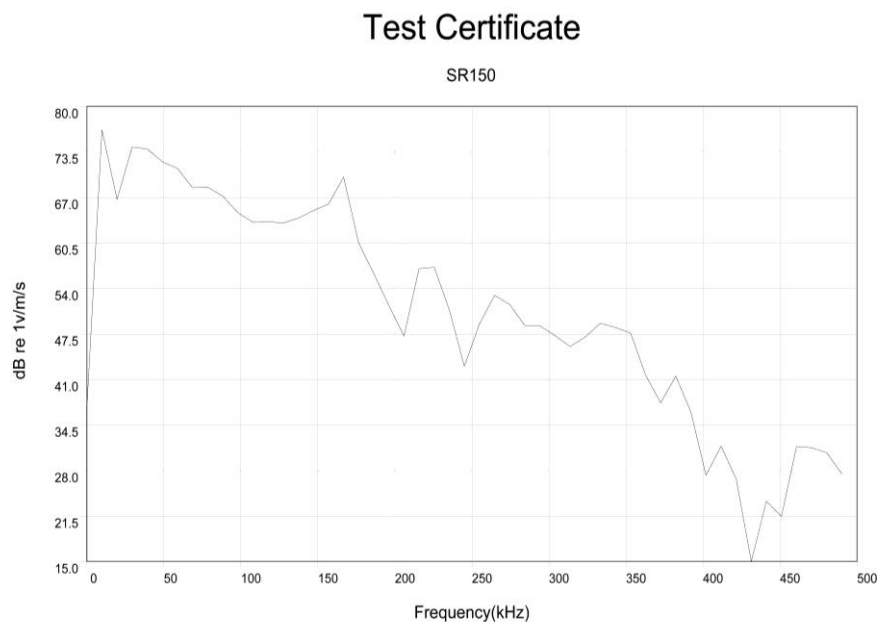## Test Certificate

### SR150



Fig. 3 The standard sensitivity curve of SR150A sensor

adopted for AE recording. Generally speaking, AE detection system is composed of the following devices with prescribed functions. A basic system is illustrated in Fig. 1. Following this system, a digital signal-processor is usually equipped.

### 2.1.1 Sensor

AE sensors are important part of the AE detection system, which should be sensitive enough to detect AE signals generated in the target structure, and be capable of converting elastic waves (motions) on the material surface into electric signals, preferably, without any distortions. Depending on the detection purpose and detection environment, AE sensors of different structures and properties should be chosen. Taking comprehensive account of various factors, the SR150A sensors were chosen in the study. The appearance and standard sensitivity curve of SR150A sensors are shown in Fig. 2 and Fig. 3 respectively.
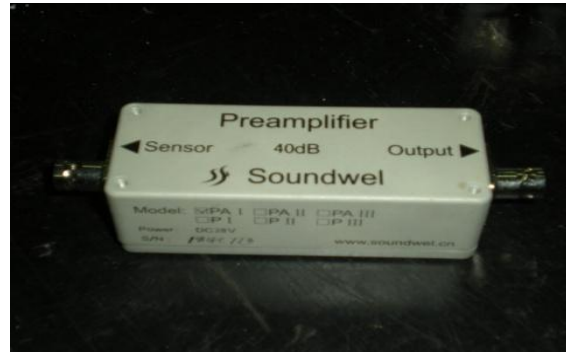
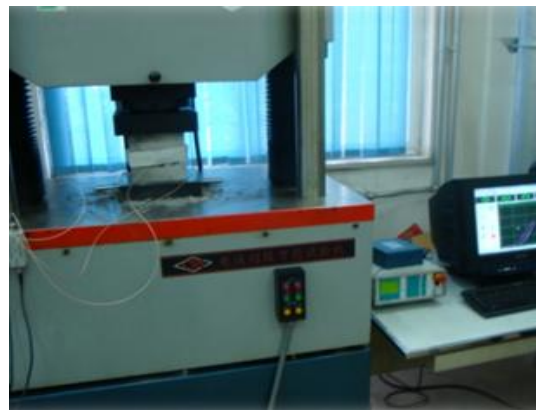Fig. 4 PAⅠstyle broadband preamplifier



Fig. 5 AE acquisition main chassis



Fig. 6 WAW-2000DL digital servo hydraulic testing system

### 2.1.2 Amplifier

In AE measuring system, amplifiers play an important role. The main function of an amplifier is to enhance signal-to-noise ratio (SNR). As the output voltage signal of sensor is always very weak, the preamplifier shall be located as close as possible to AE sensor, and the amplifiers shall be robust enough against the environmental conditions and be protected properly. In this study, the PAⅠstyle broadband preamplifier (see Fig. 4) is used. It applies to the amplification of most of AE signal.

Table 1 Type and parameter of steel fiber

| Number | Model number | Name | Type | Length (mm) | Equivalent diameter (mm) | Tensile strength (MPa) |
|--------|-------------|------|------|-------------|--------------------------|------------------------|
| 1 | hr-G03 | concave-convex | Shear indentation | 20 25 30 | 0.9 ~ 1.2 | 750 |
| 2 | hr-G01 | bow | Shear indentation | 25 30 60 | 0.9 ~ 1.2 | 900 |
| 3 | hr-G04 | Ultra short special-shaped | Shear indentation | 8-19 | 0.3 ~ 0.5 | 1100 |

(a) concave- convex          (b) bow          (c) Ultra short special-shaped

Fig. 7 Steel fibers

### 2.1.3 AEacquisition main chassis

The main chassis consists of AE acquisition card, power and case shell, as shown in Fig. 5.

### 2.2 The digital servo hydraulic testing system

To determine the strength of each type of concrete, the compressive strength tests were performed using the WAW-2000DL digital servo hydraulic testing system (see Fig. 6) in Mechanics Laboratory of China University of Geosciences (Beijing). The relative error of displayed pressure is lower than ±1%.

## 3. Experiments materials

### 3.1 Raw materials and concrete mixture

For the concrete preparation, Portland cement of 42.5 grade, medium sand, and crushed limestone of 5–20 mm continuous grading were used. Concrete mix proportion is as follows: water: cement: sand: gravel = 0.42:1:1.63:2.12.

Three types of steel fiber (see Fig. 7) are considered in this investigation, the steel fiber types and parameters are in Table 1.

### 3.2 Specimen preparation

All the specimens for flexural and fatigue test were cast in $100 \times 100 \times 100$ mm steel molds and cured in a room at 22±3℃ and95%±2% relative humidity. In order to investigate the influence of

Table 2 Number and quantity of test blocks

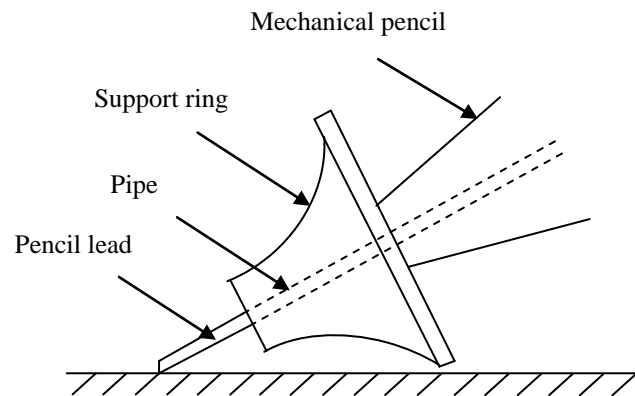| Concrete number | Volume ratio of steel fiber (%) | Steel fiber Content (g/block) |
|---|---|---|
| C0-0 | 0 | 0 |
| C1-1 | 0.5 | 39 |
| C1-2 | 1 | 78 |
| C1-3 | 1.5 | 117 |
| C2-1 | 0.5 | 39 |
| C2-2 | 1 | 78 |
| C2-3 | 1.5 | 117 |
| C3-1 | 0.5 | 39 |
| C3-2 | 1 | 78 |
| C3-3 | 1.5 | 117 |

Fig. 8 The schematic of pencil-lead break

types and mixing amounts of steel fibers on concrete compression resistance capability, four kinds of concretes including plain concrete and three types of steel fiber concretes, whose fiber volume ratios are 0.5%, 1.0% and 1.5%, respectively, as the control group have been designed. The steel fiber types and parameters are shown in Table 2.

## 4. Analysis of experiments results

### 4.1 Pencil-lead break test

Wave amplitudes exceeding a defined threshold value are referred to as AE events, and signals below the threshold value are considered as noise. In practical applications, the detection threshold was often set to 35~55dB. Because this experiment was performed in the laboratory, the noise was slight. The threshold value of 40dB was selected to ensure a high signal to noise ratio. The emitted AE signals during tests were detected by the sensors with the resonant frequency of 150 kHz. The AE signals were amplified with a 40dB gain in a preamplifier.

Table 3 Lead break test data

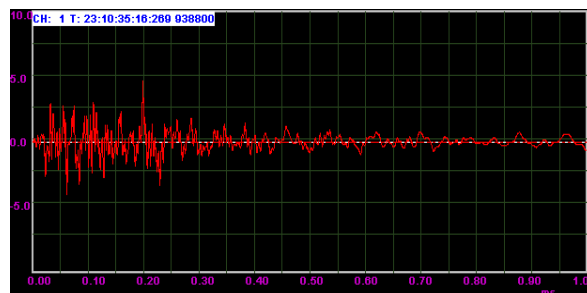| Specimen number | Rise time [µs] | Duration time [µs] |
|---|---|---|
| *1* | 197 | 530 |
| *2* | 198 | 540 |
| *3* | 198 | 525 |
| *4* | 195 | 530 |
| *5* | 201 | 550 |
| *6* | 198 | 530 |
| *7* | 197 | 545 |
| *8* | 200 | 535 |
| *9* | 196 | 535 |
| *10* | 199 | 540 |
| *average* | 197.9 | 536 |


Fig. 9 The first pencil-lead break waveform


Fig. 10 The tenth pencil-lead break waveform

Before the uniaxial compression, the pencil-lead break experiment for the C30 concrete should be done at first. The pencil-lead was about 10cm far from the sensor, and then was broken by the device shown in Fig. 8. The angel between the pencil-lead and the specimen surface was 30 degrees, and the length of the lead is about 2mm. Ten repeated tests were conducted and the average value was obtained. The results are shown in Table 3.

Owing to the limited space, only two of all waveforms are listed in Fig. 9 and Fig. 10 respectively. The average rise time is 197.9µs, and the average duration time 536µs. Therefore, the peak definition time (PDT) is set to 300µs which is about 1.5 times of the rise time, while the hit
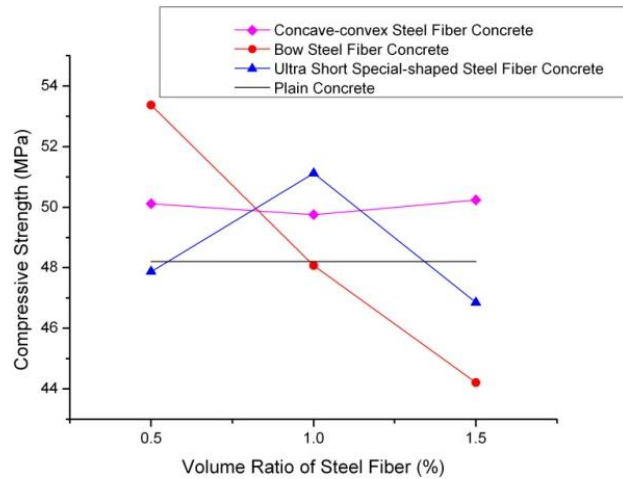
Fig. 11 Compressive strength contrast curves



|         (a)          |         (b)          |

Fig. 12 Appearance contrast figure: (a) plain concrete; (b) reinforced concrete

definition time (HDT) 800μs roughly 1.5 times of the duration time, and the hit lockout time (HLT) 1000μs which is slightly larger than HDT.

### 4.2 Compression test results

The compression test results of three kinds of steel fiber concretes with different mixing amounts and plain concrete are shown in Fig. 11.

As shown in Fig. 11 that: Convex-shaped steel fiber improves concrete compressive strength of 3% -4% in volume ratio of 0.5% -1.5%, while the mixing amount has no effect on the compressive strength in this range; compressive strength of bow steel fiber concrete decreases as volume ratio increase from 0.5% to 1.5%, and is lower than the compressive strength of plain concrete from the volume ratio of 1.0%.For ultra-short special-shaped steel fiber concrete, the compressive strength reaches the maximum when steel fiber volume ratio is 1.0%, which increases 6% comparing to plain concrete. Comparing the three kinds of steel fiber concrete and plain concrete, the compressive strength of bow steel fiber reinforced concrete reaches the maximum of 53.37MPa, which increases 10.7% compared to the compressive strength of the same strength grade of plain concrete when the steel fiber volume ratio is 0.5%.

It can be seen from the appearance (Fig. 12) that, the plain concrete shows an overall damage while the steel fiber concrete just has a surface damage. As is known to all that the failure form of
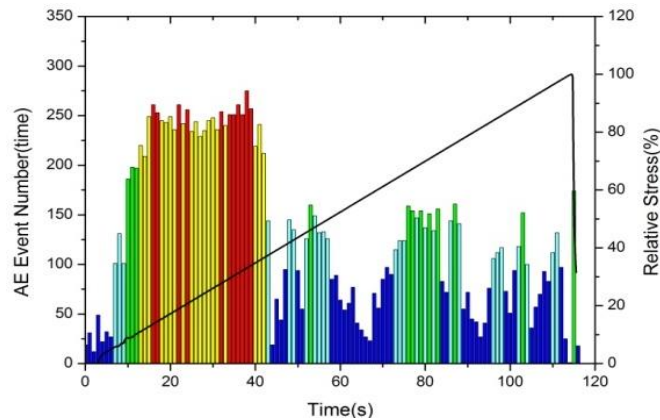
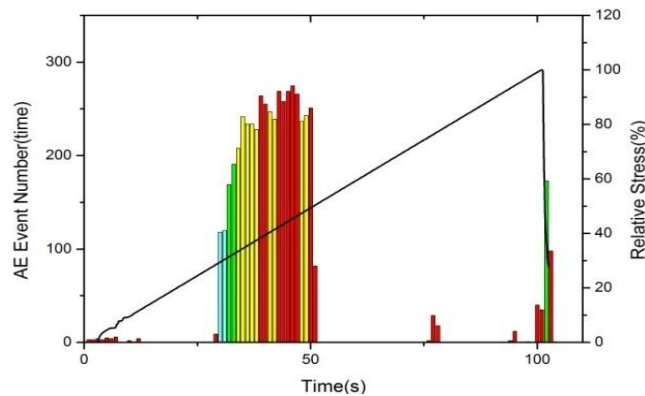Fig. 15 AE events column graphs and relative stress curves of C2-1



Fig. 16 AE events column graphs and relative stress curves of C3-1

common concrete is brittle, sudden destruction under normal circumstances. For the mixing steel fibers, however, the brittleness of concrete decreases while the ductility and toughness significantly increase. The steel fibers gradually debond and are pulled out from the concrete. Thus, steel fiber concrete shows more stable destruction state and can ensure the safety of construction better.

### 4.3 AE test results

The number of AE events per unit time is chosen to describe the acoustic emission characteristics of uniaxial compression of concrete block to reflect the frequency of concrete internal rupture events. According to test results, AE events column graphs and the relative stress curves of plain concrete and three kinds of steel fiber concrete blocks have been presented. By comparing AE signal characteristics of concrete block in different damage phases, different concrete compressive performances are reflected.

Fig. 13 is the AE events column graphs and relative stress curves of the plain concrete which acts as the control group. The contrast of AE events and relative stress curves of the three kinds of steel fiber concretes of volume ratio 0.5% are shown in Fig. 14 to Fig. 16.

From Fig. 13 to Fig. 16 it can be seen that, the AE events number of C3-1 at low stress phase (20% -30%) is less than others, which indicates that ultra-short special-shaped steel fiber can inhibit the initial crack with volume ratio of 0.5%; the AE events numbers of C1-1, C2-1, C3-1 decrease when their relative stresses are at 40% -50%, however, the AE events number of plain concrete increases, indicating that the incorporation of the three kinds of steel fiber with volume ratio of 0.5% plays a role in controlling crack propagation of concrete in later phase, although the AE events numbers of C1-1 and C3-1 are both less than that of C2-1, changes of the latter event number are more obvious, which means the first two changes significantly in internal structure, so C2-1 is better.

The contrast of AE events and relative stress curves of the three kinds of steel fiber concretes with volume ratio of 1.0% are shown in Fig. 17 to Fig. 19. From Fig. 17 to Fig. 19 it can be seen that, the AE events number of C3-2 at low stress level (20% -50%) is significantly less than that of plain concrete, the micro-cracks of ultra-short special-shaped steel fiber concrete develop lightly in early phase, meaning that this kind of steel fiber concrete has a better inhibitory effect on the generation and development of cracks in early phase with the volume ratio of 1.0%; the AE events number of C1-2, C2-2 are higher than that of plain concrete at low stress state, thus the development of initial cracks of concave-convex and bow
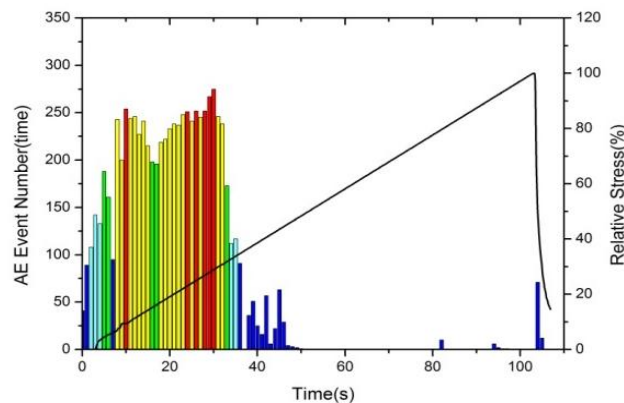


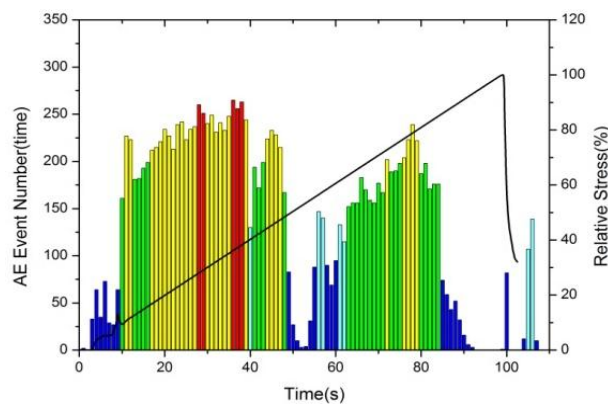Fig. 17 AE events column graphs and relative stress curves of C1-2



Fig. 18 AE events column graphs and relative stress curves of C2-2
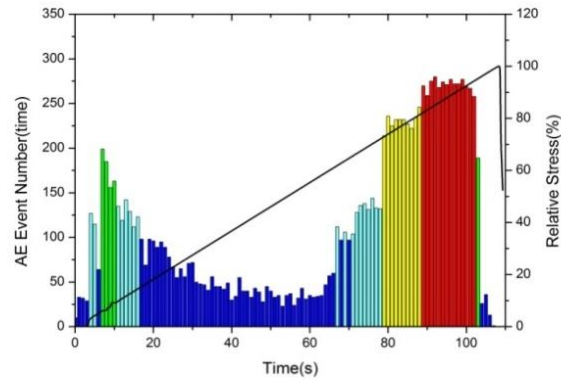
Fig. 19 AE events column graphs and relative stress curves of C3-2

steel fiber concrete are faster; after the relative stress of 40%, AE event numbers of C1-2 become smaller, even to zero, which indicates that concave-convex steel fiber of the volume ratio of 1.0% plays a role on controlling cracks in the later phase. Fu *et al*. (2014) think the steel fiber limits the crack propagation and new crack generation by weakening the stress concentration in the crack tip.
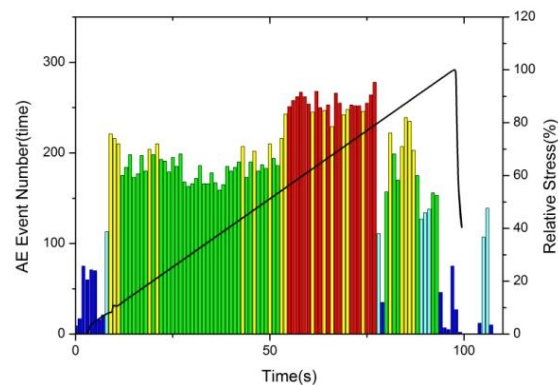


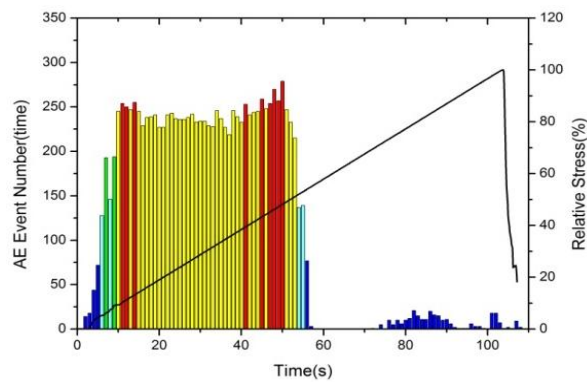Fig. 20 AE events column graphs and relative stress curves of C1-3



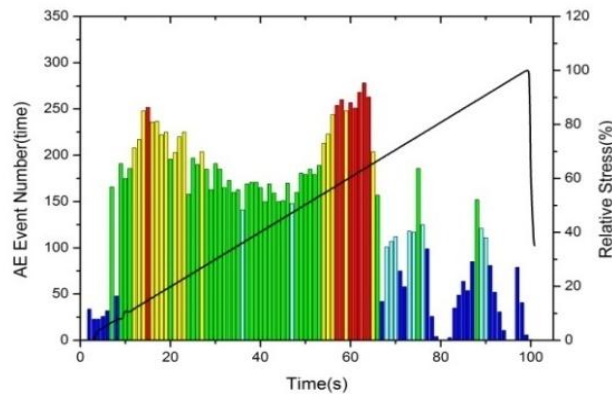Fig. 21 AE events column graphs and relative stress curves of C2-3

Fig. 22 AE events column graphs and relative stress curves of C3-3

The contrast of AE events and relative stress curves of the three kinds of steel fiber concretes with volume ratio of 1.5% are shown in Fig. 20 to Fig. 22.

From Fig. 20 to Fig. 22 it can be seen that, the AE events number of three kinds of steel fiber concretes at low stress state is higher than those in plain concrete, so early cracks of the three kinds of steel fiber concrete develop faster than plain concrete when fiber volume ratio is 1.5%; after relative stress of 50%, the AE events number of C1-3 is significantly less than that of plain concrete, after relative stress of 70%, the AE events number of C3-3 is significantly less than that of plain concrete, which indicate that concave-convex and ultra-short special-shaped steel fiber with the volume ratio of 1.5% play a part on controlling cracks in later phase.

## 5. Conclusions

Through the above analysis of selected test results, the following conclusions can be drawn:

(1) The compressive strength of concave-convex steel fiber concrete is greater than plain concrete, but when the volume ratio of steel fiber varies between 0.5% and 1.5%, the compressive strengths hardly change. AE events column graphs show that in the volume ratio between 0.5% and 1.5%, the steel fiber has an inhibitory effect on the control of crack expansion of concrete in later phase, while its internal structure changes greatly.

(2) For bow steel fiber concrete, when the volume ratio of steel fiber is 0.5%, the compressive strength is the largest of the ten groups of concrete blocks, which has an increase of 10.7% compared to that of plain concrete, and it has a better effect on the control of crack propagation of concrete in later phase. AE events column graphs show that in the volume ratio between 0.5% and 1.5%, the higher the volume ratio is, the less effective the bow steel fibers are.

(3) For ultra-short special-shaped steel fiber concrete, when the volume ratio is 1.0%, its compressive strength reaches the maximum, and 6% greater than that of plain concrete. AE events column graphs show that when the volume ratio is 1.0%, ultra-short special-shaped steel fibers play an inhibitory role on the early cracks of concrete, and the effect is better than concave-convex steel fiber which has a volume ratio of 0.5%; when the volume ratio is 0.5%, this kind of steel fiber can better control the development of crack expansion of concrete in later phase.

(4) The compressive strength and axis tensile strength are important mechanical properties of

concrete. The characteristics of acoustic emission signals in the process of axial tensile test could be researched in the future. The fatigue damage process of SFRC also can be researched by AE detection system.

## Acknowledgments

## References

Aggelis, D.G., Soulioti, D.V., Gatselou, E.A., Barkoula, N.M. and Matikas, T.E. (2013), "Monitoring of the mechanical behavior of concrete with chemically treated steel fibers by acoustic emission", *Constr. Build. Mater.*, **48**, 1255-1260.

Aggelis, D.G., Soulioti, D.V., Sapouridis, N., Barkoula, N.M., Paipetis, A.S. and Matikas, T.E. (2010), "Acoustic emission characterization of steel fibre reinforced concrete during bending", *Proceedings of SPIE-The International Society for Optical Engineering*, Spin-intSoc Optical Engineering, Bellingham, Doc n. 764912 .

Aggelis, D.G., Soulioti, D.V., Sapouridis, N., Barkoula, N.M., Paipetis, A.S. and Matikas, T.E. (2011), "Acoustic emission characterization of the fracture process in fibre reinforced concrete", *Constr. Build. Mater.*, **25**(11), 4126-4131.

Alam, S.Y., Saliba, J. and Loukili, A. (2014), "Fracture examination in concrete through combined digital image correlation and acoustic emission techniques", *Constr. Build. Mater.*, **69**(11), 232-242.

Bentahar, M. and Gouerjuma, R.E. (2009), "Monitoring progressive damage in polymer based composite using nonlinear dynamics and acoustic emission", *J. Acoust. Soc. Am.*, **125**(1), EL39-EL44.

Carpinteri, A., Corrado, M. and Lacidogna, G. (2013), "Heterogeneous materials in compression: Correlations between absorbed, released and acoustic emission energies", *Eng. Fail. Anal.*, **33**, 236-250.

Carpinteri, A., Lacidogna, G, Corrado, M, Battista, E.D. (2016), "Cracking and crackling in concrete-like materials: A dynamic energy balance", *Eng. Fract. Mech.*, **155**, 130-144.

Colombo Ing, S., Main, I.G. and Forde, M.C. (2003), "Assessing damage of reinforced concrete beam using ''b-value" analysis of acoustic emission signals", *J. Mater. Civil Eng.*, **15**(3), 280-286.

Fu, C.Q., Ma, Q.Y., Jin, X.Y., Shah, A.A. and Ye, T. (2014), "Fracture property of steel fiber reinforced concrete at early age", *Comput. Concrete*, **13**(1), 31-47.

Gholizadeh, S., Leman, Z. and Baharudin, B.T.H.T. (2015), "A review of the application of acoustic emission technique in engineering", *Struct. Eng. Mech.*, **54**(6), 1075-1095.

Ohtsu, M., Uchida, M., Okamoto, T. and Yuyama, S. (2002), "Damage assessment of reinforced concrete beams qualified by acoustic emission", *ACI Struct. J.*, **99**(4), 411-417.

Sagar, R.V. and Prasad, B.K.R. (2012), "A review of recent development in parametric based acoustic emission techniques applied to concrete structures", *Nondestruct. Test. Eval.*, **27**(1), 47-68.

Shah, A.A. and Ribakov, Y. (2011), "Recent trends in steel fibered high-strength concrete", *Mater. Des.*, **32**, (8-9), 4122-4151.

Siracusano, G., Lamonaca, F., Riccardo, T., Garescì, F., Corte, A.L., Carnì, D.L., Carpentieri, M., Grimaldi, D. and Finocchio, G. (2016), "A framework for the damage evaluation of acoustic emission signals through Hilbert-Huang transform", *Mech. Syst. Signal Process.*, **75**, 109-122.

Soulioti, D., Barkoula, N.M., Paipetis, A., Matikas, T.E., Shiotani, T. and Aggelis, D.G. (2009), "Acoustic emission behavior of steel fibre reinforced concrete under bending", *Constr. Build. Mater.*, **23**(12), 3532-3536.
Wu, K.R., Chen, B. and Wu, Y. (2000), "Study on the AE characteristics of fracture process of mortar, concrete and steel-fiber-reinforced concrete beams", *Cement Concrete Res.*, **30**(9), 1495-1500.

*CC*